Membrane and Water Treatment, *Vol. 15, No. 4 (2024) 177-183*
https://doi.org/10.12989/mwt.2024.15.4.177

Water force and the dynamics of pipes through innovative perspectives on flow and structure in fine art

Luchen Sun[1], A. Zamani Nouri*[2] and A. Yvaz[3]

[1]*School of Foreign Languages & Physical Education, Shenyang Pharmaceutical University, Liaoning Province,110016, China*
[2]*Department of Civil Engineering, Shar-e-Qods Branch, Islamic Azad University, Tehran, Iran*
[3]*World-class research center "Advanced Digital Technologies", State Marine Technical University, Saint Petersburg, 190121 Russia*

(Received July 5, 2024, Revised September 12, 2024, Accepted September 18, 2024)

Abstract. The following paper outlines the strange juncture of scientific principles and artistic expression by showing how studies of water force and dynamics of pipes can influence or inspire contemporary fine art. The radial force exerted by the internal viscous fluid is calculated using the Navier–Stokes equation. This work ascertains the fluid mechanics and structural behavior that pipes undergo due to water forces and can be translated into the medium of painting and sculpture. This paper will analyze the dynamic interactions between water and pipes reinforced with nanoparticles, while at the same time searching for new forms of representation concerning motion, flux, and structure within art. Results indicate that an increase in nanoparticle content leads to a reduction in transient deflection. The work includes case studies of artworks that incorporate these scientific aspects and also provides a theoretical framework to understand how technical phenomena can be transformed into visual and conceptual forms in art.
Keywords: dynamics; fine art; fluid and flow; pipes; water force

1. Introduction

Science and art have always had a close relationship, where artists borrow the forces of nature and mechanism to arrive at meanings of movement, structure, and form. This interplay is considered much more significant in the case of contemporary fine art, where technology introduces new materials and techniques for interpreting such forces. One such area, full of potential, is the dynamic interaction between the force of water and pipe structures. In this way, the objective is to understand exactly how the physical behavior of pipes under water pressure and fluid dynamics can inform an artistic interpretation as a means of bridging engineering principles with creative expression.

The pipes, commonly seen as functional aspects in the disciplines of civil and mechanical engineering, were new subjects viewed in a fine artistic light that showed unique insights into the laws of flow and motion. The structural dynamics of pipes under various water forces, such as internal pressure from viscous fluids and external water interactions, mirror the natural flow and resistance depicted in many forms of artistic rendition of motion. The deformation, deflection, and response of the nano-particle-reinforced pipes create fertile ground for visualizing movement within an artistic context, thus revealing the unseen forces of water into aesthetic expressions of fluidity and form. Li *et al.* (2024)

Dynamic behaviour of suspension cables due to moving loads was first investigated by Yang *et al.* in (2017). Zamanian *et al.* (2017) developed a model which analyzed the vibration and sound radiation of cylindrical shells subjected to a steady point load traveling at a rotational speed. By applying the Lagrange equation and the method of modal superposition, Pandey *et al.* (2023) have conducted an analysis of the response of orthotropic plates supported on two parallel edges due to moving loads. To analyze the dynamics of axisymmetric shells under axially moving loads, Ruzzene and Bazto (2006) resorted to FEM. An inhomogeneous Euler–Bernoulli beam with edge cracks was analytically investigated by Yang *et al.* (2017) dealing with free and forced vibrations. The work of Mosharrafian *et al.* (2016) was on the dynamic behaviour of angle-ply laminated composite plates under moving forces or masses. Mehr and Panda (2023) investigated the dynamics of an infinitely long FGM cylindrical shell due to axial tension, internal compressive loads, and moving ring-shaped pressure with constant velocity. The wave propagation, and attenuation theory has also been used by some studies to investigate steady-state vibrations in periodic pipes conveying fluid on elastic foundations with moving loads. Khelifa *et al.* (2018) studied wave propagation and attenuation theory that is used for studying the steady-state vibrations of periodic pipes on elastic foundations conveying fluid under moving loads, Berghouti *et al.* (2023) discussed simply supported uniform beams subjected to single moving point loads. The beams on nonlinear elastic foundations under moving load were investigated by Alesadi *et al.*, (2017). Applications of wave propagation in periodic Timoshenko beams on elastic foundations under constant moving loads with static axial load and structural damping were addressed by Bilouei *et al.* (2018). Dai *et al.* (2023) performed the experimental and numerical analysis

*Corresponding author, Ph.D.,
E-mail: dr.zamani.ar@gmail.com

http://www.techno-press.org/?journal=mwt&subpage=7
ISSN: 2005-8624 (Print), 2092-7037 (Online)

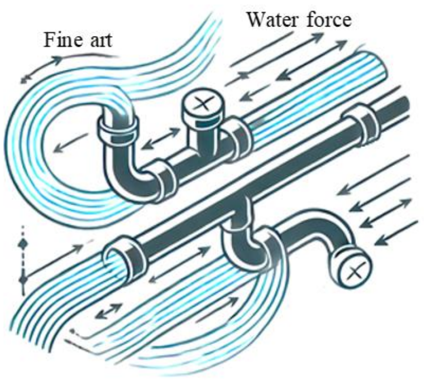

Fig. 1 A simplified scheme of water force and pipe dynamics

of ground collapse caused by underground pipeline leakage for mechanism investigation, which gives the critical insights into preventive measures. Further, Wang *et al*. (2023) have developed a permanent magnet superficial flow velocimeter that reduces output drift in flow measurement - a key factor in the management of a drainage system. These are contributions added to the development of defect feature purification by Hu *et al*. (2023). Ma *et al*. (2023) have proposed a transformer-optimized network in detecting and tracking generated defects within drainage pipelines to improve defect identification within complex environments. Yao *et al*. (2024) studied the use of a piezoresistive behavior-based method in self-sensing joints for real-time health monitoring of composite pipes to ensure timely intervention. Intelligent modeling in hydraulic transport in drainage siltation by Di *et al*. (2024), thus forming bases for some vital steps towards smarter and more resilient pipeline infrastructures.

It is in this paper that scientific logic of principles governing water force and pipe dynamics inspire new ways of creating fine art, including sculpture and painting. The technical analysis of the behavior of pipes driven by water is merged with an investigation by an artist in his quest for novel modes of visual expression of flow, structure, and resistance. This could, therefore, be said to be an interdisciplinary investigation into the expansion of understanding in dynamic forces both in structural design and the depiction and feeling of such forces within works.

2. Mode of the water in pipe with fine art

Fig. 1 is a simplified scheme of water force and pipe dynamics on a white background. It includes clean, basic shapes of the pipes both straight and curved, with arrows showing the direction of water flow and where this water presses. Black lines outline the structure of the pipes, while light blue arrows symbolize the water force that moves through them. The design emphasizes clarity and simplicity with its minimalist visual elements, depicting the interaction between water flow and pipe structure without artistic embellishment.

Based on fisrt order shell theory, the displacements are (Kolahchi *et al*. 2015, 2016a, b, Allahyari *et al*. 2024):

$$u_x(x,\theta,z,t) = u\ \ (x,\theta,t) + z\psi_x(x,\theta,t), \tag{1}$$

$$u_\theta(x,\theta,z,t) = v(x,\theta,t) + z\psi_\theta(x,\theta,t), \tag{2}$$

$$u_z(x,\theta,z,t) = w(x,\theta,t), \tag{3}$$

where u_x, u_θ, u_z are the displacements in three dirErctions; ψ_x and ψ_θ are the rotations. The strain relations are:

$$\begin{Bmatrix} \varepsilon_{xx} \\ \varepsilon_{\theta\theta} \\ \varepsilon_{x\theta} \\ \varepsilon_{xz} \\ \varepsilon_{\theta z} \end{Bmatrix} = \begin{Bmatrix} \varepsilon_{xx}^0 \\ \varepsilon_{\theta\theta}^0 \\ \varepsilon_{x\theta}^0 \\ \varepsilon_{xz}^0 \\ \varepsilon_{\theta z}^0 \end{Bmatrix} + z \begin{Bmatrix} \varepsilon_{xx}^1 \\ \varepsilon_{\theta\theta}^1 \\ \varepsilon_{x\theta}^1 \\ \varepsilon_{xz}^1 \\ \varepsilon_{\theta z}^1 \end{Bmatrix} \tag{4}$$

where

$$\begin{Bmatrix} \varepsilon_{xx}^0 \\ \varepsilon_{\theta\theta}^0 \\ \varepsilon_{x\theta}^0 \\ \varepsilon_{xz}^0 \\ \varepsilon_{\theta z}^0 \end{Bmatrix} = \begin{Bmatrix} \frac{\partial u}{\partial x} \\ \frac{\partial v}{R\partial\theta} + \frac{w}{R} \\ \frac{\partial v}{\partial x} + \frac{\partial u}{R\partial\theta} \\ \psi_x + \frac{\partial w}{\partial x} \\ \psi_\theta + \frac{\partial w}{R\partial\theta} \end{Bmatrix}, \tag{5}$$

$$\begin{Bmatrix} \varepsilon_{xx}^1 \\ \varepsilon_{\theta\theta}^1 \\ \varepsilon_{x\theta}^1 \\ \varepsilon_{xz}^1 \\ \varepsilon_{\theta z}^1 \end{Bmatrix} = \begin{Bmatrix} \frac{\partial \psi_x}{\partial x} \\ \frac{\partial \psi_\theta}{R\partial\theta} \\ \frac{\partial \psi_x}{R\partial\theta} + \frac{\partial \psi_\theta}{\partial x} \\ 0 \\ 0 \end{Bmatrix}, \tag{6}$$

The stress equations may be given as:

$$\begin{Bmatrix} \sigma_{xx} \\ \sigma_{\theta\theta} \\ \sigma_{\theta z} \\ \sigma_{zx} \\ \sigma_{x\theta} \end{Bmatrix} = \begin{bmatrix} C_{11} & C_{12} & 0 & 0 & 0 \\ C_{21} & C_{22} & 0 & 0 & 0 \\ 0 & 0 & C_{44} & 0 & 0 \\ 0 & 0 & 0 & C_{55} & 0 \\ 0 & 0 & 0 & 0 & C_{66} \end{bmatrix} \begin{Bmatrix} \varepsilon_{xx} \\ \varepsilon_{\theta\theta} \\ \gamma_{\theta z} \\ \gamma_{xz} \\ \gamma_{x\theta} \end{Bmatrix} \tag{7}$$

where C_{ij} is the elastic constants. The strain energy is:

$$U = \frac{1}{2}\int_{\Omega_0}\int_{-h/2}^{h/2} \begin{pmatrix} \sigma_{xx}\varepsilon_{xx} + \sigma_{\theta\theta}\varepsilon_{\theta\theta} + \sigma_{x\theta}\gamma_{x\theta} \\ +\sigma_{xz}\gamma_{xz} + \sigma_{\theta z}\gamma_{\theta z} \end{pmatrix} dV \tag{8}$$

With substituting Eqs. (4)-(6) into Eq. (8), we hae:

$$\begin{aligned} U = \frac{1}{2}\int_{\Omega_0} \Bigg(& N_{xx}\left(\frac{\partial u}{\partial x}\right) + N_{\theta\theta}\left(\frac{\partial v}{\partial \theta} + \frac{w}{R}\right) \\ & + Q_\theta\left(\frac{\partial w}{R\partial\theta} + \psi_\theta\right) \\ & + Q_x\left(\frac{\partial w}{\partial x} + \psi_x\right) + N_{x\theta}\left(\frac{\partial v}{\partial x} + \frac{\partial u}{R\partial\theta}\right) + M_{xx}\frac{\partial \psi_x}{\partial x} \\ & + M_{\theta\theta}\frac{\partial \psi_\theta}{R\partial\theta} + M_{x\theta}\left(\frac{\partial \psi_x}{R\partial\theta} + \frac{\partial \psi_\theta}{\partial x}\right) dx d\theta, \end{aligned} \tag{9}$$

where

$$\left(\begin{Bmatrix} N_{xx} \\ N_{\theta\theta} \\ N_{x\theta} \end{Bmatrix}, \begin{Bmatrix} M_{xx} \\ M_{\theta\theta} \\ M_{x\theta} \end{Bmatrix}\right) = \int_{-h/2}^{h/2} \begin{bmatrix} \sigma_{xx} \\ \sigma_{\theta\theta} \\ \sigma_{x\theta} \end{bmatrix} (1, z) dz \quad (10)$$

The kinetic energy for the pipe is:

$$K = \frac{\rho}{2} \int_{\Omega_0} \int_{-h/2}^{h/2} ((\dot{u}_x)^2 + (\dot{u}_\theta)^2 + (\dot{u}_z)^2)\, dV \quad (11)$$

The external work due to the fluid in the pipe is:

$$W = \int_0^L (P_{Fluid}) w dA, \quad (12)$$

where the force of fluid by Navier–Stokes equation can be give as (Bakhshandeh Amnieh *et al*. 2018, Baseri *et al*. 2016, Hajmohammad *et al*. 2021)

$$P_{fluid} = -\rho_f h_f \left(\frac{\partial^2 w}{\partial t^2} + 2\, v_x \frac{\partial^2 w}{\partial x \partial t} + {v_x}^2 \frac{\partial^2 w}{\partial x^2}\right) \quad (13)$$

where v_x and ρ_f are respectively, flow velocity and density of fluid.

The motion equations based on Hamilton's principal are:

$$\delta u: \frac{\partial N_{xx}}{\partial x} + \frac{\partial N_{x\theta}}{R\partial\theta} = I_0 \frac{\partial^2 u}{\partial t^2}, \quad (14)$$

$$\delta v: \frac{\partial N_{x\theta}}{\partial x} + \frac{\partial N_{\theta\theta}}{R\partial\theta} = I_0 \frac{\partial^2 v}{\partial t^2}, \quad (15)$$

$$\delta w: \frac{\partial Q_x}{\partial x} + \frac{\partial Q_\theta}{R\partial\theta} - \frac{N_{\theta\theta}}{R} + P_{Fluid} = I_0 \frac{\partial^2 w}{\partial t^2}, \quad (16)$$

$$\delta \psi_x: \frac{\partial M_{xx}}{\partial x} + \frac{\partial M_{x\theta}}{R\partial\theta} - Q_x = I_0 \frac{\partial^2 \psi_x}{\partial t^2}, \quad (17)$$

$$\delta \psi_\theta: \frac{\partial M_{x\theta}}{\partial x} + \frac{\partial M_{\theta\theta}}{R\partial\theta} + \frac{4}{h^2} K_\theta = I_0 \frac{\partial^2 \psi_\theta}{\partial t^2}, \quad (18)$$

where

$$I_i = \int_{-h/2}^{h/2} \rho z^i dz\, (i = 0,1,2,3), \quad (19)$$

Now, Eq. (10) can be expanded as:

$$\begin{aligned} N_{xx} &= A_{11}\left(\frac{\partial u}{\partial x}\right) + A_{12}\left(\frac{\partial v}{R\partial\theta} + \frac{w}{R}\right) + B_{11}\left(\frac{\partial \psi_x}{\partial x}\right) + B_{12}\left(\frac{\partial \psi_\theta}{R\partial\theta}\right), \\ N_{\theta\theta} &= A_{12}\left(\frac{\partial u}{\partial x}\right) + A_{22}\left(\frac{\partial v}{R\partial\theta} + \frac{w}{R}\right) + B_{12}\left(\frac{\partial \psi_x}{\partial x}\right) + B_{22}\left(\frac{\partial \psi_\theta}{R\partial\theta}\right), \\ N_{x\theta} &= A_{66}\left(\frac{\partial u}{R\partial\theta} + \frac{\partial v}{\partial x}\right) + B_{66}\left(\frac{\partial \psi_x}{R\partial\theta} + \frac{\partial \psi_\theta}{\partial x}\right), \end{aligned} \quad (20)$$

$$\begin{aligned} M_{xx} &= B_{11}\left(\frac{\partial u}{\partial x}\right) + B_{12}\left(\frac{\partial v}{R\partial\theta} + \frac{w}{R}\right) + D_{11}\left(\frac{\partial \psi_x}{\partial x}\right) + D_{12}\left(\frac{\partial \psi_\theta}{R\partial\theta}\right), \\ M_{\theta\theta} &= B_{12}\left(\frac{\partial u}{\partial x}\right) + B_{22}\left(\frac{\partial v}{R\partial\theta} + \frac{w}{R}\right) + D_{12}\left(\frac{\partial \psi_x}{\partial x}\right) + D_{22}\left(\frac{\partial \psi_\theta}{R\partial\theta}\right), \\ M_{x\theta} &= B_{66}\left(\frac{\partial u}{R\partial\theta} + \frac{\partial v}{\partial x} + \frac{\partial w}{\partial x}\frac{\partial w}{R\partial\theta}\right) + D_{66}\left(\frac{\partial \psi_x}{R\partial\theta} + \frac{\partial \psi_\theta}{\partial x}\right), \end{aligned} \quad (21)$$

where

$$A_{ij} = \int_{-h/2}^{h/2} C_{ij}\, dz, (i,j = 1,2,6) \quad (22)$$

$$B_{ij} = \int_{-h/2}^{h/2} C_{ij}\, z dz, \quad (23)$$

$$D_{ij} = \int_{-h/2}^{h/2} C_{ij}\, z^2 dz, \quad (24)$$

In the Ritz method, admissible functions are those functions satisfying the boundary conditions and utilized to approximate the displacement fields of the pipe. Then in the Ritz method, unknown functions could be expressed in a series of such admissible functions and usually taken as polynomials or trigonometric series. The description of this dynamic behavior is done by analyzing the pipe in view of the first-order shell theory that takes into account both the membrane and bending effects. Expressions for kinetic and potential energy of the pipe-fluid system will be derived, considering fluid-force interactions, geometric parameters of the pipe, and its material properties. By using the Ritz method, energy expressions are minimized with respect to the unknown coefficients of the preselected admissible functions to give a system of algebraic equations. The solution of this system furnishes the approximate displacement fields and natural frequencies of the pipe. Natural frequencies and mode shapes even of geometrically complicated pipes can be analyzed within an acceptable balance between accuracy and computational efficiency. Using this method, we have (Motezaker *et al*. 2021 a, b, Zarei *et al*. 2017):

$$[K][d(t)] + [C][\dot{d}(t)] + [M][\ddot{d}(t)] = [0] \quad (25)$$

where $[K]$ is stiffness matrix, $[C]$ is damp matrix and $[M]$ is the mass matrix. Finally, using Newmark method, the problem an be solved.

3. Numerical Results and discussion

The complex interaction of water force and piping system dynamic responses is analyzed in this paper, and an

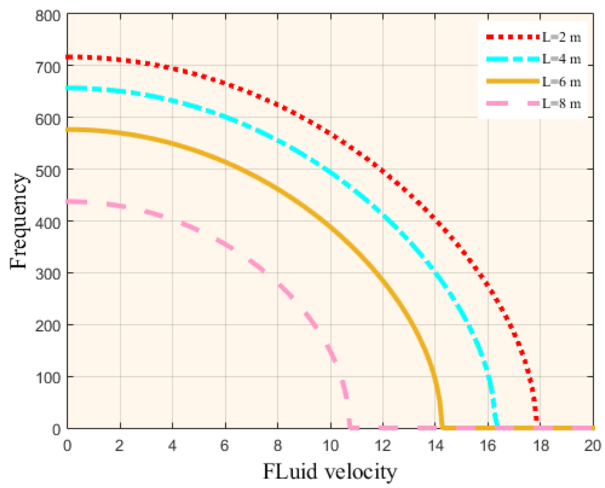

Fig. 2 Effects of pipe’s length on the frequency

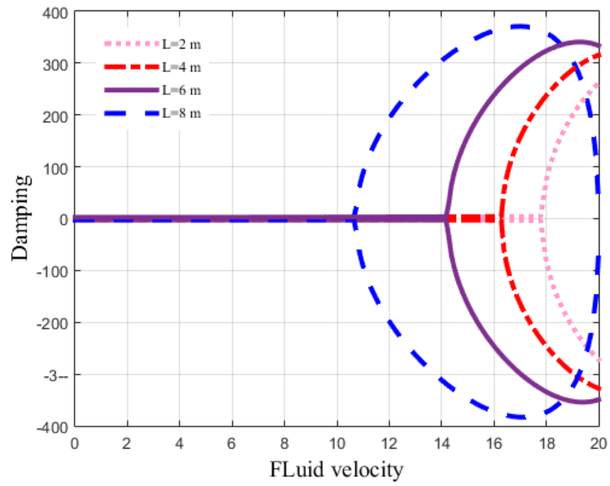

Fig. 3 Effects of pipe’s length on the damping

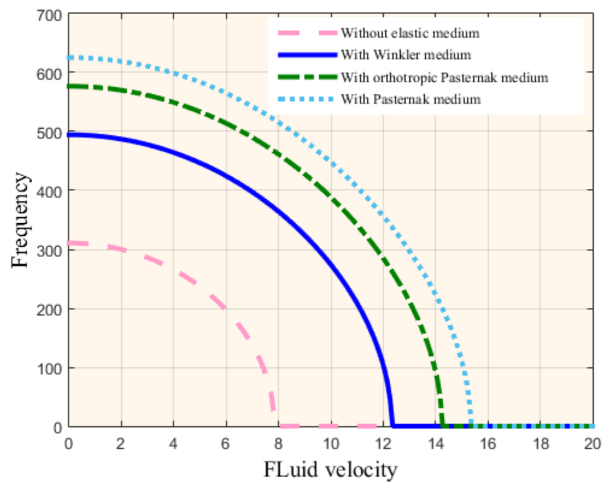

Fig. 4 Effects of elastic medium on the frequency

interdisciplinary perspective puts fluid flow in the structural design of art. Water flow influencing pipe structure will be further discussed in order to illustrate that fluid dynamics may serve in both the physical maintenance and aesthetic expression with respect to the piping systems. This research mathematically models and artistically presents the double functionality of pipes: besides carrying water, they may work as carriers of visual and conceptual creation. The research into the effects of water pressure, flow rate, and pipe curvature on structural dynamics provides a very special type of interdisciplinary-from engineering principles to those of fine art.

Figs. 2 and 3 show the effect of the pipe length on the system frequency and damping characteristic as a function of flow velocity. Stability in the pipe-fluid system is then lost at high flow velocities and results in the propensity of the piping structure against dynamic instabilities due to flutter and buckling. This is manifested in reduced stability, wherein the real and imaginary parts of the system’s natural frequency diminish correspondingly to show that the loss of stiffness increases the likelihood of resonance or failure under higher flow conditions.

It follows from the above that the imaginary part of the frequency, which is usually regarded as the damping behavior of the system, decreases with longer pipe lengths. With that, longer pipes have lower dissipation capabilities and can easily be set into full oscillations due to very high flow velocities applied to them. Finally, critical fluid velocity, which corresponds to the transition of the system from stable to unstable, also decreases with increased length. This behavior underlines the geometric sensitivity of the pipe. Indeed, longer structures are more sensitive to fluid-induced vibrations and buckling. This is due to the combined effect of reduced stiffness with a higher mass.
The consequences on the physical basis are significant. A longer pipe, though intrinsically more flexible, is seen to decline significantly in both frequency and damping, thus, it has a greater risk to carry out a catastrophic failure against dynamic fluid forces applied to the pipe. It appears then that one must pay much attention to the selection of the length of the pipe and flow conditions during the design of fluid-transport systems, particularly where stability and buckling resistance are of importance.

Figs. 4 and 5 present the dependency of pipe frequency and damping on the different surrounding media, while the effect of the elastic foundation on the dynamic response of the system is clearly presented. The inclusion of an elastic surrounding medium enhances the natural frequency of the pipe and its critical fluid velocity. This is because such an elastic foundation essentially lends more stiffness to the system, making it stronger against deformation, hence providing stability for the system under forces induced by a flowing fluid.

More precisely, the presence of an elastic medium increases the stiffness of the structural response, which in turn raises the natural frequency of the system. The natural frequency is higher because the pipe will be able to support higher fluid velocities before reaching resonance or instability. Similarly, the critical fluid velocity beyond which dynamic instabilities like flutter or buckling take place also increases with the stiffness provided by the elastic medium. This signifies that higher flow rates are achievable with the pipe without it losing stability, thereby enhancing the safety and reliability of the system in fluid transport applications.

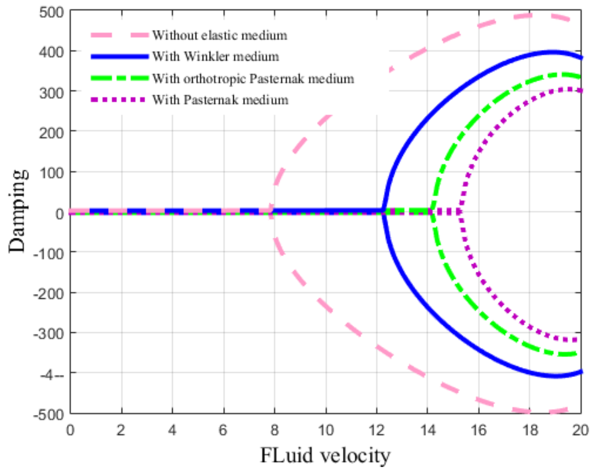

Fig. 5 Effects of elastic medium on the damping

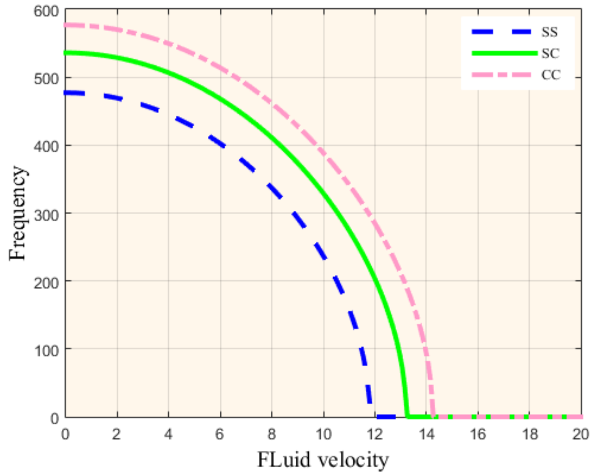

Fig. 6 Effects of boundary conditions on the frequency

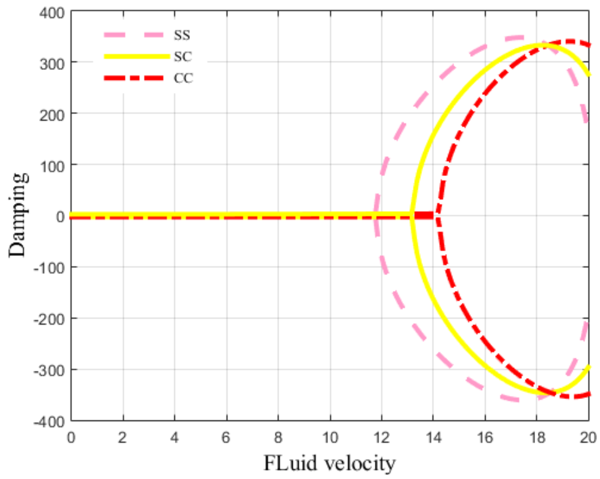

Fig. 7 Effects of boundary conditions on the damping

The comparison between the Pasternak-type and Winkler-type elastic foundations shows a stronger impact of the Pasternak model on both frequency and critical fluid velocity. The Pasternak foundation provides greater structural support, considering shear interaction between adjacent points in the medium, whereas the Winkler foundation only accounted for point-wise stiffness. Accordingly, the Pasternak foundation improves the stiffness of the pipe and stability more effectively than the others, resulting in higher values of frequency and critical flow velocity. This tends to indicate that in engineering applications where fluid-induced stability is of great importance, the type of foundation can play a decisive role in the pipe dynamics-the Pasternak model possessing the best characteristics of suppressing fluid-induced vibration and buckling.

Figs. 6 and 7 show the influence of some boundary conditions on the frequency versus damping plot of the pipe, highlighting the performance of the system dynamically subjected to these restraints. From the results, it is realized that the frequency and the critical velocity of fluid are maximum in the case of a CC boundary condition and minimum for the SS boundary condition. The variation in dynamic response exhibited by the pipe is essentially due to the amount of stiffness the structure acquires due to the different boundary conditions.

In the CC arrangement, both the pipe ends are rigidly fixed against any rotation or translational movement. As a consequence, there is a marked increase in the overall stiffness of the pipe and hence an appreciable increase in natural frequencies. A stiffer structure can resist deformation by fluid forces more effectively and hence permits a larger fluid velocity before the onset of instability. Therefore, the critical fluid velocity-beyond which dynamic instabilities such as flutter or buckling may take place-is higher in the case of CC boundary conditions. The greater rigidity of the pipe in this configuration heightens the stability of the pipe to higher flow rates.

In contrast, the simply supported (SS) arrangement provides less structural restraint because the pipe can rotate but not translate at its supports, which makes the system more flexible. Its flexibility is because the pipe resists bending and deforms under fluid forces. Consequently, this reduces the natural frequencies of the system. In terms of the critical fluid velocity for the onset of flutter, reducing the stiffness minimizes it, and hence, compared to the CC configuration, the pipe becomes susceptible to instability at smaller flow velocities.

Results highlight that boundary conditions are indeed critical in the dynamic behavior of pipes subject to fluid flow. Systems with stiffer constraints offer superior stability and performance in high-flow applications, such as in the clamped-clamped case, while less rigid systems may be more susceptible to fluid-induced vibrations and buckling. These findings are basic to the piping system design, where structural integrity coupled with resistance to dynamic instabilities becomes cardinal in high-fluid-velocity environments.

4. Conclusions

The work has given a comprehensive drive into the dynamic behaviors of pipes under the impetus of water forces within the realms of fluid mechanics and fine arts. This research, by analyzing the fluid-structure interaction through the Navier-Stokes Equation, has brought into light how such structural responses by pipes can act as an inspiring force for an artist in sculpture and painting. Focusing on pipes reinforced by nanoparticles, the results indicate that with an increase in nanoparticle content, the transient deflection decreases, hence increasing the structural stability of the system for dynamic fluid forces. Numerical results emphasize that pipe length plays an important role in stability, frequency, and damping response. Longer pipes have lower natural frequencies and reduced damping, hence, they are more susceptible to dynamic instabilities like flutter or buckling at larger flow velocities. This geometric sensitivity implies that the selection of pipe length and flow conditions is really critical in designing fluid transport systems so as to eliminate the possibility of structural failure. Again, the introduction of an elastic foundation further enhances the pipe's dynamic characteristics. The Pasternak and Winkler elastic foundations increase the natural frequency and critical fluid velocity, with the Pasternak model performing better due to the increased stiffness provided by shear interaction. This is indicative of the type of foundation playing an important role in enhancing the resistance of the pipe to fluid-induced vibrations and buckling. The boundary conditions also play a significant role in the dynamic response of the pipe. CC boundary conditions imply maximum stiffness and, hence, higher natural frequencies and critical fluid velocities, making the system more resistant to deformation and instability. Conversely, the more flexible structure provided by the SS conditions lowers the natural frequency and makes the system more vulnerable to instabilities induced by the fluid at a lower range of flow velocities.

Acknowledgments

The research is partially funded by the Ministry of Science and Higher Education of the Russian Federation as part of World-class Research Center program: Advanced Digital Technologies (contract No. 075-15-2022-312 dated 20.04.2022)

References

Allahyari, S.M.R., Shokravi, M. and Murmy, T.T. (2024), "Modeling of truncated nanocompositeconical shell structures for dynamic stability response", *Struct. Eng. Mech.*, **91**(3), 325-334. https://doi.org/10.12989/sem.2024.91.3.325.

Alesadi, A., Galehdari, M. and Shojaee, S. (2017), "Free vibration and buckling analysis of cross-ply laminated composite plates using Carrera's unified formulation based on Isogeometric approach", *Comput. Struct.*, **183**, 38-47. https://doi.org/10.1016/j.compstruc.2017.01.013.

Bakhshandeh Amnieh, H., Zamzam, M.S. and Kolahchi, R. (2018), "Dynamic analysis of non-homogeneous concrete blocks mixed by SiO2 nanoparticles subjected to blast load experimentally and theoretically", *Constr. Build. Mat.*, **174**, 633-644. https://doi.org/10.1016/j.conbuildmat.2018.04.140

Baseri, V., Jafari, G.S. and Kolahchi, R. (2016), "Analytical solution for buckling of embedded laminated plates based on higher order shear deformation plate theory", *Steel Compos. Struct.*, **21** (4), 883-919. http://doi.org/10.12989/scs.2016.21.4.883

Berghouti, H., Adda Bedia, E., Benkhedda, A. and Tounsi, A. (2023), "Vibration analysis of nonlocal porous nano- beams made of functionally graded material", *Membr. Water Treat.*, **7**(5), 351-364. http://doi.org/10.12989/mwt.2023.7.5.351.

Bilouei, B.S., Kolahchi, R. and Bidgoli, M.R., (2018), "Buckling of beams retrofitted with Nano-Fiber Reinforced Polymer (NFRP)", *Comput. Concr.*, **18**(6), 1053-1063. https://doi.org/10.12989/cac.2016.18.6.1053.

Dai, Z., Peng, L. and Qin, S. (2023), "Experimental and numerical investigation on the mechanism of ground collapse induced by underground drainage pipe leakage", *Environ. Earth Sci.*, **83**(1), 32. https://doi.org/10.1007/s12665-023-11344-w

Di, D., Li, T., Fang, H., Xiao, L., Du, X., Sun, B. and Li, B. (2024), "A CFD-DEM investigation into hydraulic transport and retardation response characteristics of drainage pipeline siltation using intelligent model", *Tunnell. Undergr. Space Technol.*, **152**, 105964. https://doi.org/10.1016/j.tust.2024.105964

Hajmohammad, M.H., Farrokhian, A. and Kolahchi, R. (2021), "Dynamic analysis in beam element of wave-piercing Catamarans undergoing slamming load based on mathematical modelling", *Ocean Eng.*, **234**, 109269. https://doi.org/10.1016/j.oceaneng.2021.109269.

Hu, C., Dong, B., Shao, H., Zhang, J. and Wang, Y. (2023), "Toward purifying defect feature for multilabel sewer defect classification", *IEEE T. Instrum. Meas.*, **72**, 1-11. http://doi.org/10.1109/TIM.2023.3250306

Khelifa, Z., Hadji, L., Hassaine Daouadji, T. and Bourada, M. (2018), "Buckling response with stretching effect of carbon nanotube-reinforced composite beams resting on elastic foundation", *Struct. Eng. Mech.*, **67**(2), 125-130. https://doi.org/10.12989/sem.2018.67.2.125.

Kolahchi, R., Bidgoli, M.R., Beygipoor, G. and Fakhar, M.H. (2015), "A nonlocal nonlinear analysis for buckling in embedded FG-SWCNT-reinforced microplates subjected to magnetic field", *J. Mech. Sci. Technol.*, **29**, 3669-3677. https://doi.org/10.1007/s12206-015-0811-9.

Kolahchi, R., Hosseini, H. and Esmailpour, M. (2016a), "Differential cubature and quadrature-Bolotin methods for dynamic stability of embedded piezoelectric nanoplates based on visco-nonlocal-piezoelasticity theories", *Compos. Struct.*, **157**, 174-186. https://doi.org/10.1016/j.compstruct.2016.08.032.

Kolahchi, R., Safari, M. and Esmailpour, M. (2016b), "Dynamic stability analysis of temperature-dependent functionally graded CNT-reinforced visco-plates resting on orthotropic elastomeric medium", *Compos. Struct.*, **150**, 255-265. https://doi.org/10.1016/j.compstruct.2016.05.023.

Li, H., Lu, H. and Li, Q. (2024), "Numerical investigations of the influences of valve spool structure on the eccentric jet flow characteristic in high-pressure angle valves", *Energy*, **298**, 131378. https://doi.org/10.1016/j.energy.2024.131378.

Ma, D., Fang, H., Wang, N., Lu, H., Matthews, J. and Zhang, C. (2023), "Transformer-optimized generation, detection, and tracking network for images with drainage pipeline defects", *Comput. Aid. Civil. Infrastr. Eng.*, **38**(15), 2109-2127. https://doi.org/10.1111/mice.12970

Mehar, K. and Panda, S.K. (2023), "Multiscale modeling approach for thermal buckling analysis of nanocomposite curved structure", *Adv. Nano Res.*, **7**(3), 181. https://doi.org/10.12989/anr.2019.7.3.181

Motezaker, M., Jamali, M and Kolahchi, R. (2021a), "Application of differential cubature method for nonlocal vibration, buckling and bending response of annular nanoplates integrated by piezoelectric layers based on surface-higher order nonlocal-piezoelasticity theory", *Comput. Appl. Math*. **369**, 112625. https://doi.org/10.1016/j.cam.2019.112625

Motezaker, M., Kolahchi, R., Rajak, D.K. and Mahmoud, S.R. (2021b), "Influences of fiber reinforced polymer layer on the dynamic deflection of concrete pipes containing nanoparticle subjected to earthquake load", *Polym. Compos.*, **42**(8), 4073-4081. https://doi.org/10.1002/pc.26118

Mosharrafian, F. and Kolahchi, R. (2016), "Nanotechnology, smartness and orthotropic nonhomogeneous elastic medium effects on buckling of piezoelectric pipes", *Struct. Eng. Mech.*, **58**(5), 931-947. https://doi.org/10.12989/sem.2016.58.5.931.

Pandey, H.K., Hirwani, C.K., Sharma, N., Katariya, P.V., Dewangan, H.C. and Panda, S.K. (2023), "Effect of nano glass cenosphere filler on hybrid composite eigenfrequency responses-An FEM approach and experimental verification", *Memb. Water Treat.*, **7**(6), 419-429. http://dx.doi.org/10.12989/mwt.2023.7.6.419.

Yang, J., Wu, H. and Kitipornchai, S. (2017), "Buckling and postbuckling of functionally graded multilayer graphene platelet-reinforced composite beams", *Compos. Struct.*, **161**, 111-118. https://doi.org/10.1016/j.compstruct.2016.11.048.

Yao, R., Ge, Z., Wang, D., Shang, N. andn Shi, J. (2024), "Self-sensing joints for in-situ structural health monitoring of composite pipes: A piezoresistive behavior- based method", *Eng. Struct.*, **308**, 118049. https://doi.org/10.1016/j.engstruct.2024.118049

Wang, Z., Wang, S., Wang, X. and Luo, X. (2023), "Permanent magnet-based superficial flow velometer with ultralow output drift", *IEEE T. Instrum. Meas.*, **72**, 1-12. https://doi.org/110.1109/TIM.2023.3304692

Zamanian, M., Kolahchi, R. and Bidgoli, M.R. (2017), "Agglomeration effects on the buckling behaviour of embedded beams reinforced with SiO2 nano-particles", *Wind. Struct.*, **24**(1), 43-57. https://doi.org/10.12989/was.2017.24.1.043.

Zarei, M.S., Kolahchi, R., Hajmohammad, M.H. and Maleki, M. (2017), "Seismic response of underwater fluid- conveying concrete pipes reinforced with SiO2 nano- particles and fiber reinforced polymer (FRP) layer", *Soil Dyn. Earthq. Eng.*, **103**, 76-85. https://doi.org/10.1016/j.soildyn.2017.09.009.

CC